Atmos. Chem. Phys. Discuss., 9, 17937–17962, 2009
www.atmos-chem-phys-discuss.net/9/17937/2009/


Atmospheric Chemistry and Physics Discussions

This discussion paper is/has been under review for the journal *Atmospheric Chemistry and Physics (ACP)*. Please refer to the corresponding final paper in *ACP* if available.

# Annual cycle of ozone at and above the tropical tropopause: observations versus simulations with the Chemical Model of the Stratosphere (CLaMS)

**P. Konopka[1], J.-U. Grooß[1], G. Günther[1], F. Plöger[1], R. Pommrich[1], R. Müller[1], and N. Livesey[2]**

[1]Forschungszentrum Jülich (ICG-1: Stratosphere), Germany
[2]Jet Propulsion Laboratory, California Institue of Technology, Pasadena, CA, USA

Received: 10 July 2009 – Accepted: 10 August 2009 – Published: 1 September 2009

Correspondence to: P. Konopka (p.konopka@fz-juelich.de)

Published by Copernicus Publications on behalf of the European Geosciences Union.





## Abstract

Multi-annual simulations with the Chemical Model of the Stratosphere (CLaMS) are used to study the seasonality of $O_3$ and of the mean age within the stratospheric part of the tropical tropopause layer (TTL) In agreement with satellite (HALOE) and in-situ observations (SHADOZ), CLaMS simulations show above ≈360 K potential temperature, a pronounced annual cycle in $O_3$ and in the mean age of air with highest values in the late boreal summer. Within the model, this seasonality is driven by the seasonality of both upwelling and in-mixing. The latter process describes enhanced meridional transport from the extratropics into the TTL. The strongest in-mixing occurs from the Northern Hemisphere during the boreal summer in the potential temperature range between 380 and 420 K. Contrary, an increase of upwelling with highest values in winter reduces $O_3$ up to the lowest values in early spring. Both, CLaMS simulations and Aura MLS $O_3$ observations show that this enhanced equatorward transport in summer is mainly driven by the Asian monsoon anticyclone.

## 1 Introduction

A quantitative understanding of transport across the tropical tropopause layer (TTL) which is acting as a "gateway to the stratosphere" plays a key role in determining the stratospheric concentrations of water vapor and other chemical species (Fueglistaler et al., 2009). The TTL which roughly extends between 350 and 420 K vertically, is laterally confined by the subtropical jets (STJ) which vary seasonally both in their intensity and meridional position. (e.g. Haynes and Shuckburgh, 2000; Konopka et al., 2007; Fueglistaler et al., 2009)

An imminent consequence of transport across the TTL is the composition of air within the TTL that shows a strong seasonality. In particular,at the tropical tropopause (i.e. $p$≈100 hPa or $\theta$≈380 K, $p$-pressure, $\theta$-potential temperature), high water vapor ($H_2O$), high ozone ($O_3$), low carbon monoxide (CO) during summer (seasons are



ACPD

9, 17937–17962, 2009



related to the Northern Hemisphere) alternate with low $H_2O$, low $O_3$ and high CO during winter (Folkins et al., 2006; Schoeberl et al., 2006; Randel et al., 2007).

In this work, we focus on the seasonality of $O_3$, in particular on the question how far the isentropic transport from the extra-tropics into stratospheric part of the TTL, i.e. roughly above the level of zero clear sky radiation ($\theta \approx 360$ K), contributes to the observed annual cycle of $O_3$ above the tropical tropopause, in particular to a pronounced maximum in summer (Randel et al., 2007). In the following we briefly refer to this kind of transport as in-mixing. The seasonality of $O_3$ is exemplary shown in Fig. 1 where the observations of the Southern Hemisphere ADditional OZonesondes (SHADOZ) network (Thompson et al., 2007) are used to determine the fractional annual cycle of $O_3$ in the tropics, $\Delta O_3/\langle O_3\rangle$, ($\langle O_3\rangle$ – annual mean, $\Delta O_3 = O_3 - \langle O_3\rangle$). In the derivation of the seasonal cycle of $O_3$ we follow the procedure described in Randel et al. (2007) but instead of pressure we use potential temperature as the vertical coordinate. In particular, $p$-related observations are transformed to $\theta$-levels using the measured temperatures and these results are averaged over the seven closest station to the equator.

Thus, a clear annual cycle of $\Delta O_3/\langle O_3\rangle$, with highest values of $\Delta O_3/\langle O_3\rangle$ in late summer and early fall in the $\theta$-range between 370 and 430 K, can be diagnosed from the SHADOZ data. The lowest values appear approximately 6 month earlier. The pattern of this very pronounced cycle is very similar to the analysis on $p$-levels (Chae and Sherwood, 2007; Randel et al., 2007), although $\Delta O_3/\langle O_3\rangle$ is significantly smaller (0.5 versus 0.3 during summer by using $p$ and $\theta$ as the vertical coordinate, respectively) (Fueglistaler et al., 2009; Konopka et al., 2009). As discussed by Konopka et al. (2009), a significant part of the variability of $\Delta O_3/\langle O_3\rangle$ on $p$-levels is a seasonal adiabatic process (as $p$-levels move relative to the $\theta$-levels during the year) that can be removed by using potential temperature $\theta$ as the vertical coordinate.

The seasonality of $O_3$ above the level of zero clear sky radiative heating ($Q$=0), i.e. roughly above $\theta$=360 K level (Gettelman et al., 2004), was recently explained as a consequence of the annual cycle in the tropical upwelling with strongest and weakest upwelling in winter and summer, respectively (Randel et al., 2007). Randel et al. (2007)



ACPD
9, 17937–17962, 2009



also showed that this annual cycle of upwelling is approximately in phase with the well-known seasonal variation of the tropical temperatures with highest (lowest) temperatures during the summer (winter). In their analysis, Randel et al. (2007) assumed that tropics are well-isolated from the extra-tropics, i.e. that the horizontal in-mixing from the extratropics into the TTL is negligible. Recently, Schoeberl et al. (2008) followed the same arguments in order to explain the fluctuations in tropical trace gases observed by HALOE and Aura MLS instruments within the TTL.

However, as our previous study based on the HALOE and SHADOZ observations of $O_3$ and on a simple conceptual model of transport and photochemistry shows (Konopka et al., 2009), the observed seasonality of $O_3$ on $\theta$-levels, with highest values during boreal summer, can not be understood solely by photolytical $O_3$ production in slowly rising air masses which are well-isolated from the extratropics. By quantifying the photochemical production of $O_3$ in ascending air and by using the SHADOZ climatology to estimate the tropospheric $O_3$ mixing ratio, Konopka et al. (2009) determined the residual variability in observed $O_3$ and interpreted this residuum as being caused by horizontal in-mixing from the extratropical stratosphere.

Evidences of quasi-horizontal (i.e. isentropic) in-mixing into the TTL are not new (e.g. Volk et al., 1996; Avallone and Prather, 1997; Folkins et al., 1999). Using ozone sondes and aircraft observations of $N_2O/O_3$ correlations, signatures of stratospheric contributions were found within the TTL above 14 km and well below the tropopause, indicating this region as a transition zone separating the troposphere from the stratosphere (Tuck et al., 1997). Recently, Marcy et al. (2007) showed that more than 60% of their airborne in situ HCl observations within the TTL (up to ≈100 pptv below $\theta$≈390 K) have stratospheric origin and that this HCl is well-correlated with $O_3$.

Using the Chemical Lagrangian Model of the Stratosphere (CLaMS) (McKenna et al., 2002; Konopka et al., 2007), we discuss here how well the annual cycle of $O_3$ above the tropical tropopause derived from satellite (HALOE) and in situ observations (SHADOZ) can be reproduced by this model. Whereas most of the published model studies on this topic are based on conceptual 2D-models, where the meridional transport is



ACPD
9, 17937–17962, 2009



not well-resolved and mostly neglected (see e.g. Read et al. (2008) and the citations therein), we show within a full 3-D study that the isentropic in-mixing significantly influences the composition of the lower tropical stratosphere, in particular that of $O_3$ in summer. We also show that the summer Asian monsoon anticyclone drives such horizontal in-mixing of sub- and extra-tropical air masses into the stratospheric part of the TTL.

## 2 The configuration of CLaMS

Multi-annual, global CLaMS simulations of the whole troposphere and stratosphere (from the ground up to $\theta$=2500 K) follow the model set-up described by Konopka et al. (2007) and cover the time period from October 2001 to December 2005 with 100 km horizontal resolution and the highest vertical resolution of 400 m around $\theta$=380 K. The horizontal winds are driven by the European Centre for Medium-Range Weather Forecast (ECMWF) operational analysis.

Above 100 hPa, potential temperature $\theta$ acts as the vertical coordinate of the model and the cross-isentropic velocity $\dot{\theta}$ is derived from a radiation calculation using the Morcrette scheme under clear sky conditions (Morcrette, 1991). Below 100 hPa the model smoothly transforms from $\theta$ to hybrid potential temperature $\zeta$ (Mahowald et al., 2002), and gradually includes the large-scale vertical velocity from ECMWF ($\Omega$=$\dot{p}$).

The concept of the hybrid vertical velocity, $\dot{\zeta}$ discussed in Konopka et al. (2007) mixes below $p$=100 hPa the ECMWF vertical velocity $\dot{p}$ with $\dot{\theta}$ derived from the clear-sky radiation calculation. Because this definition violates mass conservation, we correct this velocity by a latitude-dependent factor (cosine-weighted between ±50°N and constant below and above $\theta$=360 K, respectively) at each $\theta$-level chosen in such a way that the annually averaged mass conservation is fulfilled (Rosenlof, 1995). In the following, we show mainly CLaMS results obtained with the corrected vertical velocity (default case) but discuss also their differences with respect to the vertical velocity described in (Konopka et al., 2007) (reference case).



ACPD
9, 17937–17962, 2009



To illustrate how these two alternatives drive the upwelling within the TTL, the seasonality of $\dot{\theta}$, derived from $\dot{\theta}=\dot{\zeta}(d\theta/d\zeta)$ and averaged over the 2002-05 period is shown in Fig. 2.

In the left panel, the zonal and latitudinal (±10°N) average of $\dot{\theta}$ (corrected case) is plotted as a function of $\theta$ and season whereas the annual mean is shown in the right panel (black and red line for $\dot{\theta}$ in K/d and mm/s, dashed and solid for the reference and the corrected case, respectively. The velocity $w$ in mm/s was inferred from $\dot{\theta}$ in K/d using $w=\dot{\theta}\cdot dz/d\theta$ with $dz/d\theta$ from the tropical climatology (Randel et al., 2007)).

Compared to the vertical velocity used in Konopka et al. (2007), the corrected vertical velocity enhances the mean tropical upwelling below the tropopause and removes the gap of the negative velocities around $\theta$=350 K which are causing the violation of the annually averaged mass conservation (the upper and lower edge of this gap are denoted by two thick and dashed white lines). Furthermore, the corrected vertical velocity also slightly decreases the upwelling above $\theta$=360 K towards values which agree fairly well with the upwelling estimated from the upward propagation of the tape-recorder signals (Mote et al., 1998; Niwano et al., 2003) estimated to be of the order 0.3 mm/s at $\theta$=450 K (thick green dashed vertical line in the right panel of Fig. 2)

Thus, the part of the TTL around $\theta$=360 K, with smallest mean upwelling, couples the convection-dominated troposphere (semi-annual cycle of $\dot{\theta}$) with the radiation-dominated stratosphere (annual cycle of $\dot{\theta}$). According to Konopka et al. (2007), not only the vertical but also the horizontal (isentropic) transport, although strongly triggered by Rossby and Kelvin waves, is also influenced by mixing. Thus, in addition to the advective part of transport (horizontal and vertical velocities), the vertical and isentropic mixing determine the composition of air within the TTL.

## 3 CLaMS simulations

The species transported in CLaMS are: $O_3$, $pO_3$ (passive ozone) and the mean age. For the chemistry of $O_3$, only photolytical ozone production and the $HO_x$-driven $O_3$ loss



ACPD
9, 17937–17962, 2009



cycle in the lower stratosphere are considered. The OH concentrations are prescribed from a climatology. Passively transported ozone ($pO_3$, i.e. $O_3$ without chemistry) allows the contribution of transport to be estimated, in particular that of in-mixing. $O_3$ and $pO_3$ within the boundary layer (the lowest model layer) are set to zero. Because of this simplified chemistry all APs above $\theta$=500 K are prescribed by the HALOE climatology (Grooß and Russell, 2005). In this way $O_3$ and $pO_3$ are only calculated between the Earth surface (both set to zero) and $\theta$=500 K (both set to HALOE climatology) and can be understood as a result of transport, photo-chemistry and $HO_x$-driven $O_3$ loss cycles whereas the chemistry (of $O_3$) mainly acts in the tropics above $\theta$=360 K.

The mean age of air is calculated from the time lag relative to a linear increasing source within the boundary layer (Waugh and Hall, 2002). The mean age at $\theta$=2500 K is derived from Michelson Interferometer for Passive Atmospheric Sounding (MIPAS) observations of $SF_6$ (Stiller et al., 2008). A perpetuum run of the first year (10 times from 1 October 2001 to 30 September 2002) defines a steady state of the model that is used here as the initial state.

The seasonality of $O_3$ at $\theta$=380 K derived from CLaMS (2002-05) and from the the 10-year climatology of the Halogen Occultation Experiment (HALOE) (Grooß and Russell, 2005) is shown in the top and bottom panels of Fig. 3, respectively.

Some differences between CLaMS and HALOE are obvious, in particular on the Southern Hemisphere where the contribution of the ozone hole is not reproduced in CLaMS (no halogen-induced chemistry in this version of CLaMS). However, generally a strong similarity in the seasonal pattern of the tropical $O_3$ can be diagnosed for both data sets, in particular the clear maximum of HALOE $O_3$ between July and November around the equator is reproduced fairly well by CLaMS.

These enhanced values of $O_3$ in late summer near the equator simulated in CLaMS correlate reasonably well with enhanced values of $pO_3$ and of the mean age (Fig. 4).

Because $pO_3$ is set to 0 at the Earth's surface, the enhanced values of $pO_3$ can only originate from the stratosphere. Furthermore, a permanent upwelling above the $Q$=0 level, i.e. above ≈360 K excludes downward transport within the tropics as a possible



ACPD
9, 17937–17962, 2009



source of $pO_3$. Thus, $pO_3$ can be understood as a measure of horizontal in-mixing from the extratropics into the TTL.

This interpretation is further supported by enhanced values of the mean age (bottom panel of Fig. 4) indicating that older air masses are mixed into the TTL around the tropical tropopause during summer. Thus, horizontal in-mixing from the Northern Hemisphere extra-tropics rather than photolytical production explains the summer maximum of ozone at $\theta$=380 K. In the next section we discuss this finding more quantitatively by comparing SHADOZ and HALOE observations of $O_3$ with CLaMS results.

## 4 CLaMS versus observations

To compare CLaMS results with observations more quantitatively, we plot in Fig. 5, the seasonality of $O_3$ on $\theta$-levels extending between 360 and 420 K. Here, SHADOZ observations are shown (beige) and CLaMS simulations are determined on the geographical locations of the considered seven SHADOZ stations (red and black for $O_3$ and $pO_3$, respectively). The dashed and solid lines are derived form the reference and corrected CLaMS run, respectively. The gray line denotes the seasonality of $O_3$ obtained from the HALOE climatology (Grooß and Russell, 2005) averaged within the latitude range ±10°N. The vertical lines around the SHADOZ data show the total variability between the considered seven stations.

The difference between the $O_3$ and $pO_3$ time series is a measure of the chemical $O_3$ production and, as expected, the contribution of the photolytically formed $O_3$ grows with increasing altitude. Furthermore, the shape of the seasonality derived from CLaMS agrees fairly well with the SHADOZ and HALOE observations above $\theta$=360 K, in particular all time series show a clear maximum in late summer.

A remarkable feature of CLaMS time series is that $O_3$ and $pO_3$ show exactly the same seasonality with a pronounced maximum in summer and a much weaker second maximum around February. Moreover, the percentage of $pO_3$ compared with the total simulated $O_3$ is around 50% at $\theta$=380 K indicating that, at least in the model, transport



ACPD
9, 17937–17962, 2009



rather than chemical production determines not only the seasonality of the $O_3$ cycle but also a significant part of the ozone budget.

As we discuss in the next sections, the maximum of $O_3$ between August (380 K) and October (420 K) as derived from the SHADOZ observations is strongly connected to an enhanced meridional, equatorward transport into the stratospheric part of the TTL during summer. On the other side, the weaker winter maximum diagnosed in the model is hardly present in the HALOE/SHADOZ observations. In CLaMS this signal results from an enhanced equatorward transport from the Southern Hemisphere during austral summer.

Thus, although CLaMS overestimates the semi-annual cycle of $O_3$ the model results fairly agree with the observations at $\theta$-levels above 360 K. Contrary, the observed time series at $\theta$=360 K show a much weaker seasonality than CLaMS. A strong station-to-station variability of the SHADOZ data, in particular up to 360 K, is much higher than the corresponding variability of the CLaMS time series (not shown). Here, CLaMS underestimates the variability of the convection-driven transport, at least at the location of the considered SHADOZ stations. This is plausible because below 100 hPa CLaMS uses the large-scale ECMWF vertical winds which do not sufficiently include the effect of the localized convection that can deeply penetrate into the stratosphere (Ricaud et al., 2007). Furthermore, there is no tropospheric $O_3$-production in the model that is expected to be driven by hydrogen and nitrogen radicals (Wennberg et al., 1998) and requires a very detailed (and hardly available) information on the atmospheric composition.

## 5 In-mixing and the Asian monsoon anticyclone

The importance of isentropic in-mixing for the composition of air around the tropical tropopause can also be deduced from the horizontal distribution of the mean age at $\theta$=380 K shown in Fig. 4. Here, a clear difference of the zonal winds (from thick to thin white lines are plotted for 20, 15 and 10 m/s, respectively) between the Northern



ACPD
9, 17937–17962, 2009



and Southern Hemisphere (NH and SH) is obvious. On both hemispheres the STJ is weaker during the respective summer than during the respective winter (Chen, 1995) with smallest zonal winds on the NH in summer. The STJ on the SH forms an effective transport barrier during the whole year even if some weaker signatures of in-mixing from the SH can be seen during NH winter (see enhanced $pO_3$ and mean age in February, March at 20°S).

The most pronounced hemispheric asymmetry of the climatological flow pattern in the vicinity of the tropopause originates from the Asian summer monsoon that manifests as a strong anticyclone in the upper troposphere (Dethof et al., 1999; Randel and Park, 2006; Park et al., 2007). This nearly stationary summer circulation extends well into the lower stratosphere up to about 20 km (or $\theta$=420 K) and effectively isolates the air masses of tropospheric origin inside from much older, mainly stratospheric air outside of this anticyclone (Park et al., 2008). Furthermore, this circulation significantly weakens the STJ making it permeable for meridional transport (Haynes and Shuckburgh, 2000).

In Fig. 6 the horizontal distribution of $O_3$ at $\theta$=380 K is shown for the winter months, December to February (DJF, left) and summer months, June to August (JJA, right) derived from the CLaMS simulations (corrected case, 2002-05, top) and observations measured by the Microwave Limb Sounder (MLS) on the NASA Earth Observing System (EOS) Aura (Schoeberl et al., 2006) (bottom). The MLS profiles (Version 2.2) sampled between August 2004 and December 2008 were first interpolated on the model $\theta$-levels (using ECMWF temperature) and than, both CLaMS data and MLS observations, were averaged within 250×250 km bins. The precision and the uncertainty of MLS data amounts to 40 and 50 ppbv at 100 hPa, respectively (Livesey et al., 2008).

The comparison between the CLaMS and the MLS data shows that although very similar pattern are resolved by both data sets, the $O_3$ mixing ratios measured by MLS are slightly higher than the corresponding CLaMS values (with exception of the SH in DJF where CLaMS overestimates MLS due to missing of the halogen-induced $O_3$ loss forming the ozone hole and propagating downwards in austral summer). Although the



ACPD
9, 17937–17962, 2009



absolute difference increases towards the poles, the relative difference is of the order 20% in rough agreement with the relative accuracy of the MLS retrieval discussed in Livesey et al. (2008) (these differences become even smaller than 10% if the CLaMS data are averaged over three isentropic levels, 370, 380, and 400 K in order to mimic the averaging kernel of the MLS instrument, not shown).

Nevertheless, the similarity of the patterns between MLS and CLaMS, with lowest $O_3$ values over the equator in winter and with a clear signature of the Asian monsoon anticyclone in summer confirms the seasonal patterns of transport resolved by CLaMS. In particular, the summer distribution of $O_3$ shows a very pronounced wave-2 structure with highest values of $O_3$ in the eastern flank of the Asian monsoon and over Central America. Whereas the Asian monsoon anticyclone is also obvious in the wind pattern, it is not clear to what extent the second maximum over Central America is driven by the North American monsoon.

For an aqua-planet with negligible tropospheric sources of $O_3$ one expects that summer and winter $O_3$-distributions are symmetric to each other. However, the real atmosphere shows an annual cycle in the tropical upwelling that is approximately anticorrelated to the well-known seasonal variation of the tropical temperatures, i.e. slowest and fastest upwelling occurs during the summer and winter, respectively (Randel et al., 2007). Thus, the question arises if the discussed seasonality of $O_3$ with a clear maximum in late summer is solely a consequence of the seasonality of the tropical upwelling or if also in-mixing, mainly in summer from the NH (Asian monsoon), significantly influences this pattern.

## 6 Discussion

Based on a simple conceptual model of transport and photochemistry Konopka et al. (2009) argued that the observed seasonality of $O_3$ with highest values during boreal summer, can not be understood only by photolytical $O_3$ production in slowly rising air masses which are well-isolated from the extratropics. Utilizing CLaMS we can



ACPD
9, 17937–17962, 2009



determine the contribution of in-mixing to the calculated seasonality of $O_3$. In particular, the use of the passively transported $O_3$, $pO_3$, allows the impact of horizontal transport to be quantified more precisely.

Because $pO_3$ (and also $O_3$) is set to the HALOE climatology for $\theta$>500 K (upper boundary) and to 0 at the Earth surface (lower boundary), only transport from the stratosphere can enhance $pO_3$ within the TTL. In particular, because upwelling with persistent positive (upward) values of $\dot{\theta}$ determines transport above $Q$=0 level (≈360 K), only horizontal in-mixing can transport $pO_3$ into the TTL. The numerical vertical diffusion has also some potential to produce "undesirable" vertical transport but this effect would not change the seasonality of $pO_3$. Moreover, sensitivity studies (not shown) with artificial tracers initialized above $\theta$=420 K within ±10°N latitude range show that downward transport driven by the numerical diffusion is negligible. Contrary, if there were no horizontal in-mixing into the TTL, $pO_3$ would be zero and, consequently, the seasonal pattern of $pO_3$ measures in CLaMS the amount of isentropically transported $O_3$ into the TTL.

A remarkable result of CLaMS simulations is the percentage of $pO_3$ compared with the total $O_3$ (see Fig. 7).

Here, the fraction $pO_3/(O_3+O_{3trop})$ was derived from the model using reference (top) and corrected (bottom) vertical velocity. In addition we assume that $O_{3trop}$=40 ppbv for the contribution of the tropospheric $O_3$ flux (in CLaMS the lower boundary of $O_3$ is set to 0). With this assumption $O_3+O_{3trop}$ roughly reproduces the SHADOZ climatology at $\theta$=360 K. Thus, Fig. 7 clearly shows a strong enhancement (up to 40% and 60% for the reference and corrected cases, respectively) of the contribution of in-mixing during late summer and early fall within the $\theta$-range between 360 and 420 K. In particular, the relative minimum of in-mixed $O_3$ to the total $O_3$ occurs in spring.

Note that CLaMS simulations with the mass-corrected vertical velocity enhance (reduce) upwelling below (above) $\theta$≈360 K level if compared with the reference run. Consequently, $pO_3$ and also the fraction $pO_3/(O_3+O_{3trop})$ show a related signature, with lower and higher values below and above ≈360 K, respectively. Because the



ACPD
9, 17937–17962, 2009



corrected vertical velocity not only remove the the gap in upwelling discussed in Konopka et al. (2007) but also reproduce better the $H_2O$ tape-recorder and the tropical $CH_4$ profiles (not shown), the corresponding higher values of in-mixed $O_3$ shown in the bottom panel of Fig. 7 are probably more reliable results of our investigations.

An interesting feature of both the cycle of $\Delta O_3/\langle O_3 \rangle$ (Fig. 1) and of the cycle of in-mixing (Fig. 7) is that their maxima (or minima) occur in late summer and fall (or spring), i.e. approximately 2–3 months later than the weakest (or strongest) vertical transport can be diagnosed in the ECMWF data (see left panel of Fig. 2). This property can be qualitatively explained by the fact that it needs some time to fill or to dilute the TTL with respect to $O_3$. In other words, the maximum or minimum of $O_3$ appears about 2–3 months after the strongest horizontal transport from the NH in summer and the strongest vertical transport from the troposphere in winter fill and dilute the TTL with $O_3$, respectively. In addition, the semi-annual cycles of convection (below 360 K) and of in-mixing (probably overestimated in CLaMS) also modulate this phase difference.

All these findings support our analysis based on a simple conceptional model (Konopka et al., 2009) that transport rather than chemistry drives the tropical seasonality of $O_3$ in this part of the atmosphere. Supplementary to the analysis of Randel et al. (2007), not only the annual cycle of the vertical velocity but also the seasonality of in-mixing is important to obtain the observed time series. Summarized, in-mixing enhances $O_3$ in summer and upwelling dilutes $O_3$ in winter within the TTL extending between 360 and 420 K – this scenario is at least strongly motivated by our studies.

The origin of enhanced in-mixing can be traced back to a strongly disturbed zonal flow on the Northern Hemisphere in summer, mainly by the persistent Asian monsoon anticyclone (wave-2 pattern, see Fig. 6), in qualitative agreement with some idealized, isentropic studies of transport (Chen, 1995; Plumb, 1996; Haynes and Shuckburgh, 2000). Such enhanced meridional transport in summer is also obvious in pure trajectory calculations driven by the ERA-Interim horizontal winds and temperature tendencies (Plöger et al., 2009).



ACPD
9, 17937–17962, 2009



In addition, the zonally averaged meridional velocities indicate that the equatorward horizontal advection in summer from NH overweigh the advective transport from the SH in winter (not shown). Thus, the seasonality of $pO_3$ (i.e. of in-mixing) is driven by the advective part of transport rather than by mixing. This can be confirmed also by CLaMS simulations where mixing was switched off (pure trajectory transport) where the same seasonality of $pO_3$ was diagnosed.

Finally, sensitivity studies with CLaMS driven be the ERA-Interim winds with vertical wind derived from the temperature tendencies (Fueglistaler et al., 2008; Plöger et al., 2009) show that although if the absolute values of in-mixing (i.e. of $pO_3$) depend on the used winds (mainly on the vertical winds), the presented seasonality of $O_3$ is a very robust feature of our simulations. Due to the fact that the ECMWF-based vertical velocities do not resolve deep, overshooting convection that, as recently discussed by Ricaud et al. (2007), contributes to enhanced values of CO, $CH_4$, $N_2O$, mainly over Africa during the spring season, CLaMS probably overestimates the impact of horizontal in-mixing on the composition of the TTL.

## 7 Conclusions

Multi-annual simulations with the the Chemical Model of the Stratosphere (CLaMS) suggest that the impact of the northern extra-tropics in summer, in particular in connection with the summer Asian monsoon, significantly influences the composition of air within the TTL between 360 and 420 K potential temperature. Our study also shows that the picture of a TTL, "well-isolated" from the extratropics, should be revised, in particular between 360 and 440 K, by a picture where both the annual cycle of upwelling *and horizontal in-mixing* determine the seasonality of $O_3$ and of other relevant species within the TTL.



ACPD
9, 17937–17962, 2009



*Acknowledgements.* Excellent programming support was provided by N. Thomas. We also thank W. J. Randel for many discussions motivating the authors to conduct this study and to write this paper. We are also grateful to Mijeong Park for providing us with SHADOZ-based $O_3$-climatology. Work at the Jet Propulsion Laboratory, California Institute of Technology, was carried out under a contract with the National Aeronautics and Space Administration. The European Centre for Medium-Range Weather Forecasts (ECMWF) provided meteorological analyses for this study.

## References

Avallone, L. M. and Prather, M. J.: Tracer-tracer correlations: Three-dimensional model simulations and comparisons to observations, J. Geophys. Res., 102, 19233–19246, 1997. 17940

Chae, J. H. and Sherwood, S. C.: Annual temperature cycle of the tropical tropopause: A simple model study, J. Geophys. Res., 112, 1–10, 2007. 17939

Chen, P.: Isentropic cross-tropopause mass exchange in the extratropics, J. Geophys. Res., 100, 16661–16673, 1995. 17946, 17949

Dethof, A., O'Neill, A., Slingo, J. M., and Smit, H. G. J.: A mechanism for moistening the lower stratosphere involving the Asian summer monsoon, Q. J. Roy. Meteorol. Soc., 556(125), 1079–1106, 1999. 17946

Folkins, I., Loewenstein, M., Podolske, J., Oltmans, S. J., and Proffitt, M.: A barrier to vertical mixing at 14 km in the tropics: Evidence from ozonesondes and aircraft measurements, Geophys. Res. Lett., 104, 22095–22102, 1999. 17940

Folkins, I., Bernath, P., Boone, C., Lesins, G., Livesey, N., Thompson, A. M., Walter, K., and Witte, J. C.: Seasonal cycles of $O_3$, CO, and convective outflow at the tropical tropopause, Geophys. Res. Lett., 33, L16802, doi:10.1029/2006GL026602, 2006. 17939

Fueglistaler, S., Legras, B., Beljaars, A., Morcrette, J.-J., Simmons, A., Tompkins, A. M., and Uppapla, S.: The diabatic heat budget of the upper troposphere and lower/mid stratosphere in ECMWF reanalysis, Q. J. Roy. Meteorol. Soc., 110, 1–27, doi:10.1002/qj.000, 2008. 17950

Fueglistaler, S., Dessler, A. E., Dunkerton, T. J., Folkins, I., Fu, Q., and Motte, P. W.: Tropical tropopause layer, Rev. Geophys., *RG1004*, doi:10.1029/2008RG000267, 2009. 17938, 17939

Gettelman, A., de F. Fujiwara, P. M., Fu, Q., Vömel, H., Gohar, L. K., Johanson, C., and





Aaammerman, M.: Radiation balance of the tropical tropopause layer, J. Geophys. Res., 109(D07103), doi:10.1029/2003JD004190, 2004. 17939
Grooß, J.-U. and Russell III, J. M.: Technical note: A stratospheric climatology for $O_3$, $H_2O$, $CH_4$, $NO_x$, HCl and HF derived from HALOE measurements, Atmos. Chem. Phys., 5, 2797–2807, 2005, http://www.atmos-chem-phys.net/5/2797/2005/. 17943, 17944, 17958, 17960
Haynes, P. and Shuckburgh, E.: Effective diffusivity as a diagnostic of atmospheric transport, 2, Troposphere and lower stratosphere, J. Geophys. Res., 105, 22795–22810, 2000. 17938, 17946, 17949
Konopka, P., Günther, G., Müller, R., dos Santos, F. H. S., Schiller, C., Ravegnani, F., Ulanovsky, A., Schlager, H., Volk, C. M., Viciani, S., Pan, L. L., McKenna, D.-S., and Riese, M.: Contribution of mixing to upward transport across the tropical tropopause layer (TTL), Atmos. Chem. Phys., 7, 3285–3308, 2007, http://www.atmos-chem-phys.net/7/3285/2007/. 17938, 17940, 17941, 17942, 17949, 17957
Konopka, P., Grooß, J.-U., Plöger, F., and Müller, R.: Annual cycle of horizontal in-mixing into the TTL, J. Geophys. Res., in press, 2009. 17939, 17940, 17947, 17949
Livesey, N. J., Filipiak, M. J., Froidevaux, L., Read, W. G., Lambert, A., Santee, M. L., Jiang, J. H., Pumphrey, H. C., Waters, J. W., Cofield, R. E., Cuddy, D. T., Daffer, W. H., Drouin, B. J., Fuller, R. A., Jarnot, R. F., Jiang, Y. B., Knosp, B. W., Li, Q. B., Perun, V. S., Schwartz, M. J., Snyder, W. V., Stek, P. C., Thurstans, R. P., Wagner, P. A., Avery, M., Browell, E. V., Cammas, J.-P., Christensen, L. E., Diskin, G. S., Gao, R.-S., Jost, H.-J., Loewenstein, M., Lopez, J. D., Nedelec, P., Osterman, G. B., Sachse, G. W., and Webster, C. R.: Validation of Aura Microwave Limb Sounder $O_3$ and CO observations in the upper troposphere and lower stratosphere, J. Geophys. Res., 113, D15S02, doi:10.1029/2007JD008805, 2008. 17946, 17947
Mahowald, N. M., Plumb, R. A., Rasch, P. J., del Corral, J., and Sassi, F.: Stratospheric transport in a three-dimensional isentropic coordinate model, J. Geophys. Res., 107(D15), 4254, doi:10.1029/2001JD001313, 2002. 17941
Marcy, T. P., Popp, P. J., Gao, R. S., Fahey, D. W., Ray, E. A., Richard, E. C., Thompson, T. L., Atlas, E. L., Loewenstein, M., Wofsy, S. C., Park, S., Weinstock, E. M., Swart, W. H., and Mahoney, M. J.: Measurements of trace gases in the tropical tropopause layer, Atmos. Environ., 41, 7253–7261, 2007. 17940
McKenna, D. S., Konopka, P., Grooß, J.-U., Günther, G., Müller, R., Spang, R., Offer-





mann, D., and Orsolini, Y.: A new Chemical Lagrangian Model of the Stratosphere (CLaMS): 1. Formulation of advection and mixing, J. Geophys. Res., 107(D16), 4309, doi:10.1029/2000JD000114, 2002. 17940

Morcrette, J.-J.: Radiation and Cloud Radiative Properties in the European Centre for Medium-Range Weather Forecasts Forecasting System, J. Geophys. Res., 96(D5), 9121–9132, 1991. 17941

Mote, P. W., Dunkerton, T. J., McIntyre, M. E., Ray, E. A., Haynes, P. H., and Russell III, J. M.: Vertical velocity, vertical diffusion, and dilution by midlatitude air in the tropical lower stratosphere, J. Geophys. Res., 103, 8651–8666, 1998. 17942, 17957

Niwano, M., Yamazaki, K., and Shiotani, M.: Seasonal and QBO variations of ascent rate in the tropical lower stratosphere as inferred from UARS HALOE trace gas data, J. Geophys. Res., 108(D24), 4794, doi:10.1029/2003JD003871, 2003. 17942, 17957

Park, M., Randel, W. J., Emmons, L. K., Bernath, P. F., Walker, K. A., and Boone, C. D.: Chemical isolation in the Asian monsoon anticyclone observed in Atmospheric Chemistry Experiment (ACE-FTS) data, J. Geophys. Res., 112(D16309), doi:10.1029/2006JD008294, 2007. 17946

Park, M., Randel, W. J., Emmons, L. K., Bernath, P. F., Walker, K. A., and Boone, C. D.: Chemical isolation in the Asian monsoon anticyclone observed in Atmospheric Chemistry Experiment (ACE-FTS) data, Atmos. Chem. Phys., 8, 757–764, 2008, http://www.atmos-chem-phys.net/8/757/2008/. 17946

Plöger, F., Konopka, P., Günther, G., Grooß, J.-U., and Müller, R.: Impact of the vertical velocity scheme on modeling transport across the tropical tropopause layer, J. Geophys. Res., submitted, 2009. 17949, 17950

Plumb, R. A.: A "tropical pipe" model of stratospheric transport, J. Geophys. Res., 101, 3957–3972, 1996. 17949

Randel, W. J. and Park, M.: Deep convective influence on the Asian summer monsoon anticyclone and associated tracer variability observed with Atmospheric Infrared Sounder (AIRS), J. Geophys. Res., 111, D12314, doi:10.1029/2005JD006490, 2006. 17946

Randel, W. J., Park, M., Wu, F., and Livesey, N.: A large annual cycle in ozone above the tropical tropopause linked to the Brewer-Dobson circulation, J. Atmos. Sci., 64, 4479–4488, 2007. 17939, 17940, 17942, 17947, 17949, 17956

Read, W. G., Schwartz, M. J., Lambert, A., Su, H., Livesey, N. J., Daffer, W. H., and Boone, C. D.: The roles of convection, extratropical mixing, and in-situ freeze-drying in the Tropical





Tropopause Layer, Atmos. Chem. Phys., 8, 6051–6067, 2008, http://www.atmos-chem-phys.net/8/6051/2008/. 17941

Ricaud, P., Barret, B., Attié, J.-L., Motte, E., Le Flochmoën, E., Teyssèdre, H., Peuch, V.-H., Livesey, N., Lambert, A., and Pommereau, J.-P.: Impact of land convection on troposphere-stratosphere exchange in the tropics, Atmos. Chem. Phys., 7, 5639–5657, 2007, http://www.atmos-chem-phys.net/7/5639/2007/. 17945, 17950

Rosenlof, K. H.: Seasonal cycle of the residual mean meridional circulation in the stratosphere, J. Geophys. Res., 100, 5173–5191, 1995. 17941

Schoeberl, M. R., Kawa, S. R., Douglass, A. R., Waters, J., Livesey, N., Read, W., and Filipiak, M.: The carbon monoxide tape recorder, Geophys. Res. Lett., 33, L12811, doi:10.1029/2006GL026178, 2006. 17939, 17946

Schoeberl, M. R., Douglass, A. R., Newman, P. A., Lait, L. R., Lary, D., Waters, J., Livesey, N., Froidevaux, L., Lambert, A., Read, W., Filipiak, M. J., and Pumphrey, H. C.: QBO and annual cycle variations in tropical lower stratosphere trace gases from HALOE and Aura MLS observations, J. Geophys. Res., 113, D05301, doi:10.1029/2007JD008678, 2008. 17940

Stiller, G. P., von Clarmann, T., Höpfner, M., Glatthor, N., Grabowski, U., Kellmann, S., Kleinert, A., Linden, A., Milz, M., Reddmann, T., Steck, T., Fischer, H., Funke, B., López-Puertas, M., and Engel, A.: Global distribution of mean age of stratospheric air from MIPAS SF6 measurements, Atmos. Chem. Phys., 8, 677–695, 2008, http://www.atmos-chem-phys.net/8/677/2008/. 17943

Thompson, A. M., Witte, J. C., Smit, H. G. J., Oltmans, S. J., Johnson, B. J., Kirchhoff, V. W., and Schmidlin, F. J.: Southern Hemisphere Additional Ozonesondes (SHADOZ) 1998–2004 tropical ozone climatology: 3. Instrumentation, station-to-station variability, and evaluation with simulated flight profiles, J. Geophys. Res., 112(D03304), 1297–1300, doi:10.1029/2005JD007042, 2007. 17939, 17956

Tuck, A. F., Baumgardner, D., Chan, K. R., Dye, J. E., Elkins, J. W., Hovde, S. J., Kelly, K. K., Loewenstein, M., Margitan, J. J., May, R. D., Podolske, J. R., Proffitt, M. H., Rosenlof, K. H., Smith, W. L., Webster, C. R., and Wilson, J. C.: The Brewer-Dobson circulation in the light of high altitude in situ aircraft observation, Q. J. Roy. Meteorol. Soc., 123, 1–69, 1997. 17940

Volk, C. M., Elkins, J. W., Fahey, D. W., Salawitch, R. J., Dutton, G. S., Gilligan, J. M., Proffitt, M. H., Loewenstein, M., Podolske, J. R., Minschwaner, K., Margitan, J. J., and Chan, K. R.: Quantifying transport between the tropical and mid-latitude lower stratosphere, Science, 272, 1763–1768, 1996. 17940



ACPD

9, 17937–17962, 2009



Waugh, D. W. and Hall, T. M.: Age of stratospheric air: Theory, observations, and models, Rev. Geophys., 40(4), 1–27, 2002. 17943

Wennberg, P. O., Hanisco, T. F., Jaegle, L., Jacob, D. J., Hintsa, E. J., Lanzendorf, E. J., Anderson, J. G., Gao, R. S., Keim, E. R., Donnelly, S. G., Del Negro, L. A., Fahey, D. W., MsKeen, S. A., Salawitch, R. J., Webster, C. R., May, R. D., Herman, R. L., Proffitt, M. H., Margitan, J. J., Atlas, E. L., Schauffler, S. M., Flocke, F., McElroy, C. T., and Bui, T. P.: Hydrogen Radicals, Nitrogen Radicals, and the Production of $O_3$ in the Upper Troposphere, Science, 279, 49–53, 1998. 17945





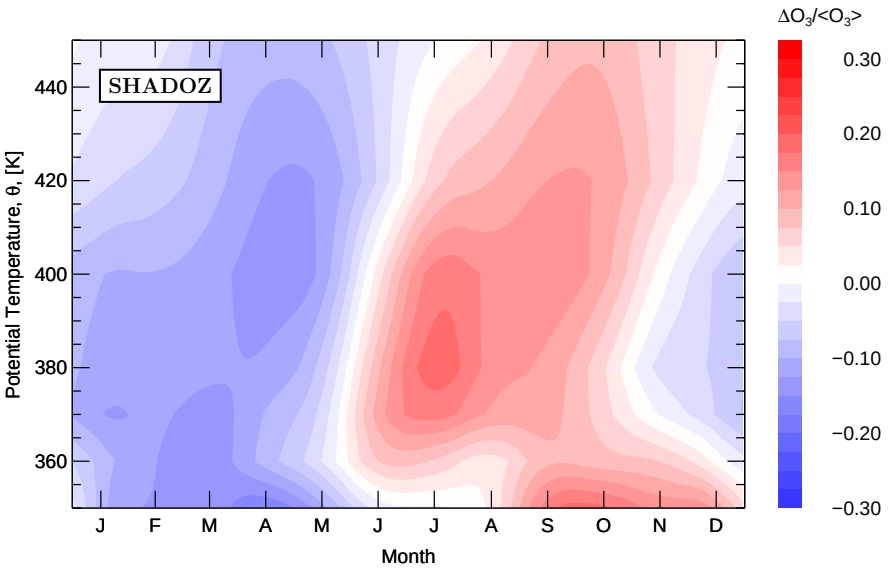


**Fig. 1.** The fractional annual cycle of $O_3$ in the tropics, $\Delta O_3/\langle O_3\rangle$, ($\langle O_3\rangle$ – annual mean, $\Delta O_3 = O_3 - \langle O_3\rangle$.) averaged over the seven SHADOZ station which are closest to the equator (Thompson et al., 2007; Randel et al., 2007).



ACPD
9, 17937–17962, 2009



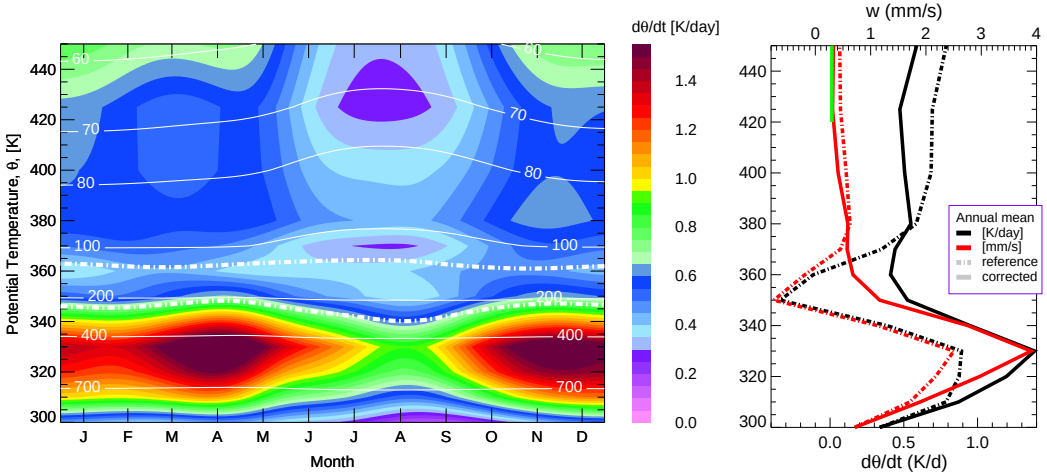


**Fig. 2.** Left: Seasonality of the upwelling in CLaMS described in term of $\dot{\theta}$ averaged zonally and within the ±10°N range during the 2002-05 period (corrected case). White thin lines are isobars. Above $p$=100 hPa, $\dot{\theta}$ results from the clear sky radiation, below $p$=100 hPa, the contribution of the clear sky radiation to $\dot{\theta}$ is gradually replaced by the ECMWF vertical velocity. The thick dashed lines are $\dot{\theta}$=0 isolines of the reference case described in Konopka et al. (2007). Right: The corresponding annual mean (solid) compared with the reference case (dashed). Black and red lines denote $\dot{\theta}$ in K/d and mm/s, respectively. The thick green dashed vertical line approximate the upwelling at $\theta$=450 K with $w \approx 0.3$ mm/s derived the upward propagation of the tape-recorder signal (Mote et al., 1998; Niwano et al., 2003)).



ACPD
9, 17937–17962, 2009

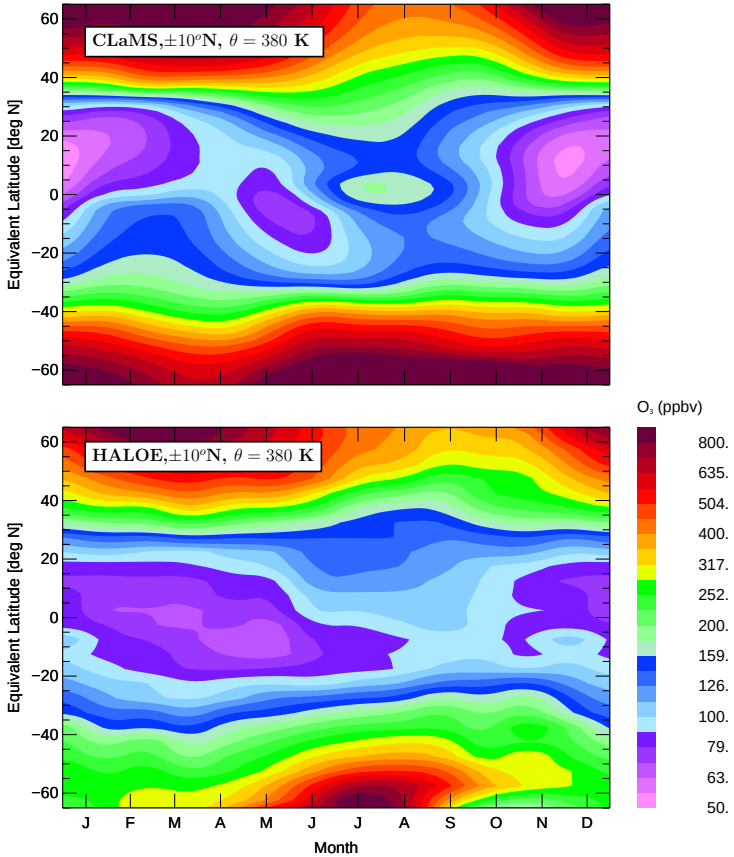


**Fig. 3.** The seasonality of $O_3$ at $\theta$=380 K. Top: From CLaMS (2002-05). Bottom: From the 10-year HALOE climatology (Grooß and Russell, 2005).



ACPD
9, 17937–17962, 2009

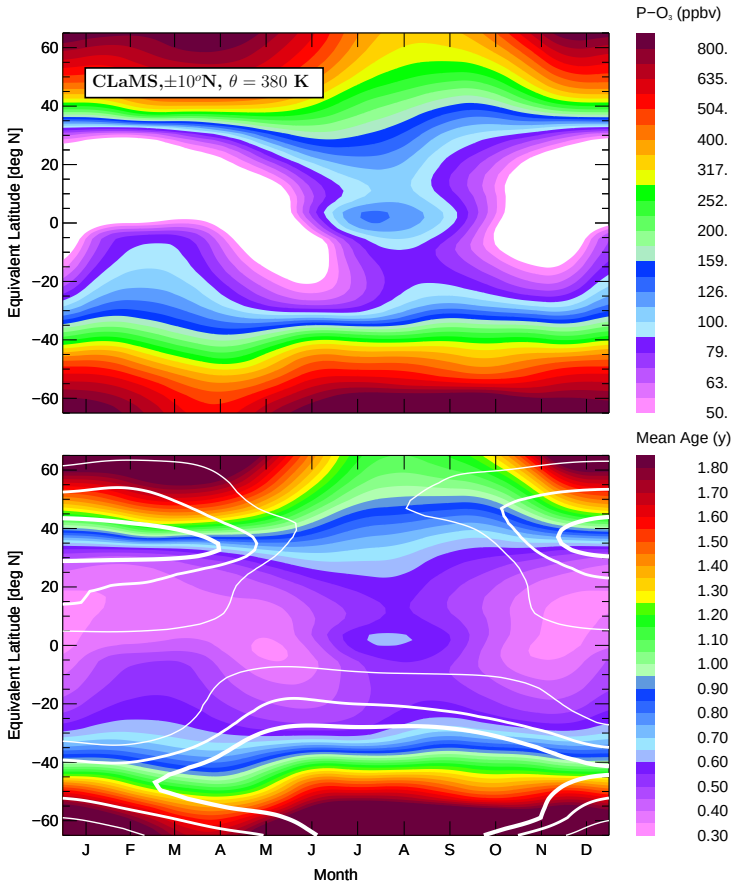


**Fig. 4.** The seasonality of passively transported $O_3$ ($pO_3$, top) and of the mean age of air (bottom) at $\theta$=380 K as derived from CLaMS. The white lines are isolines of the horizontal wind plotted for 20, 15 and 10 m/s (from thick to thin).



ACPD
9, 17937–17962, 2009

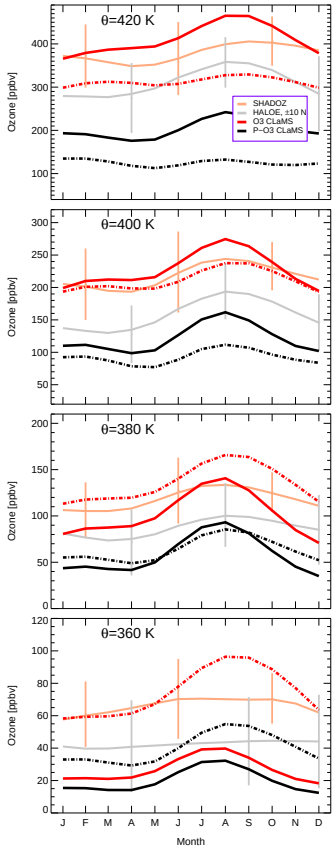


**Fig. 5.** Seasonality of the SHADOZ observations (seven closest station to the equator, beige) versus CLaMS deduced time series of $O_3$ and $pO_3$ (red and black, dashed – reference, solid – corrected) at $\theta$-levels 360, 380, 400, and 420 K (from bottom to top). In the case of the SHADOZ data, the beige vertical lines describe the total variability between the considered seven stations. In addition, $O_3$ from the HALOE climatology (Grooß and Russell, 2005) averaged within the latitude range ±10°N with corresponding standard deviation (vertical lines) is shown (gray).



ACPD
9, 17937–17962, 2009



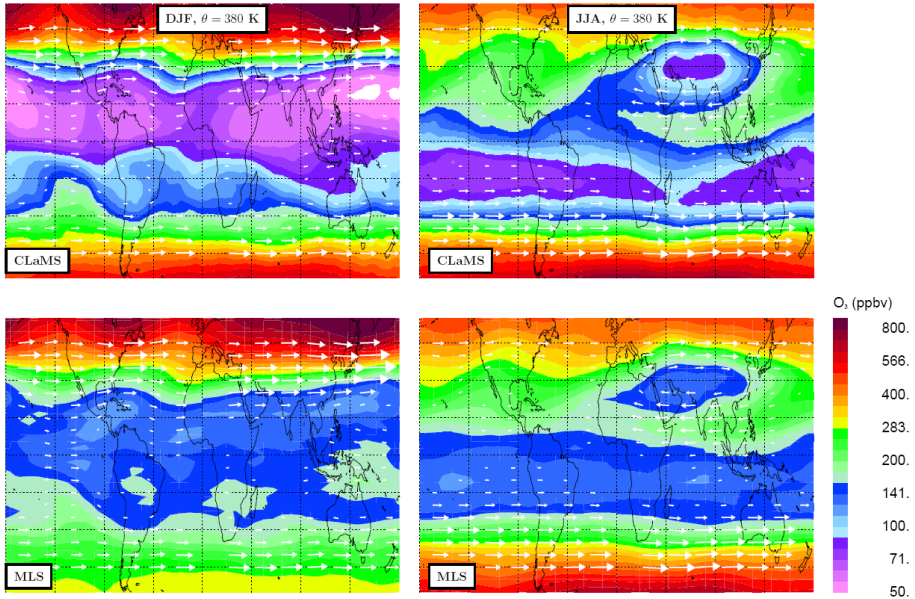


**Fig. 6.** Mean distribution of $O_3$ at $\theta$=380 K as calculated with CLaMS (top) and derived from Aura MLS observations (bottom, Version 2.2) during the winter (DJF, left) and summer (JJA, right). For CLaMS and MLS the averaged values over the 2002-05 and 2005-07 periods, respectively, were calculated. The white arrows denote the isentropic wind derived from ECMWF data covering the 2002-05 period.



ACPD
9, 17937–17962, 2009

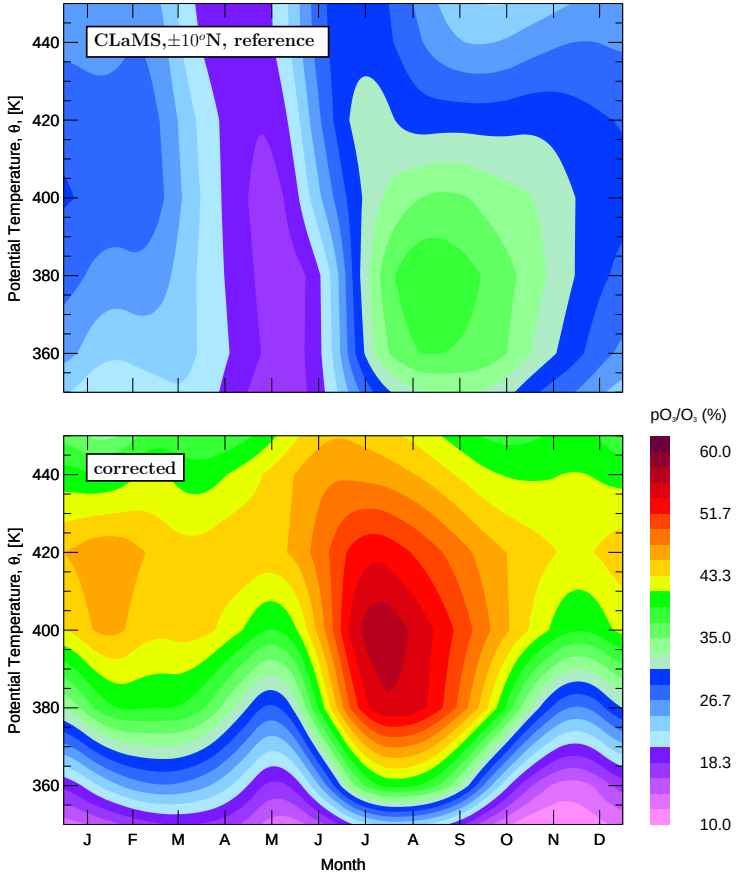


**Fig. 7.** Contribution of in-mixing calculated from CLaMS as fraction $pO_3/(O_3+O_{3trop})$. $O_{3trop}$ describes the $O_3$ flux from the troposphere that was assumed to 40 ppbv (in CLaMS this contribution is neglected due to the condition $O_3$=0 at the Earth surface). Top and bottom panels show CLaMS results for the reference and for the corrected case, respectively.



ACPD
9, 17937–17962, 2009